

# Numerical Solutions for Transient Electromagnetic Field in Rectangular Bus Bars

Alin DOLAN, Grigore A. CIVIDJIAN

University of Craiova, Electrical Engineering Faculty, Decebal Bvd. 107, Craiova, Romania, 200440;  
adolan@elth.ucv.ro

**Abstract.** The transient electromagnetic field in and around a system of two non-magnetic homogenous rectangular bars is evaluated with finite element method. The influence of mesh quality on the solution accuracy is discussed. For high-enough bars, a combined analytical-numerical solution for the field penetration in the bar and for the time variation of the current density distribution is proposed and comparison with purely numerical solutions is made.

## 1 Introduction

The transitory electromagnetic field problem in two infinite-high and long non-magnetic bars is completely analytically solved in [1], considering the magnetic field on external side of the bars equal to zero. In [2] these results were extended for the case of finite but high-enough bars, maintaining the assumption of one-dimensional field in central part of the bar, constantly distributed on the height and considering the external magnetic field no more zero. In this paper a numerical solution is obtained with finite element method using FLUX program at current step injection and voltage step application to short-circuited high-enough bars. The results are compared with the old analytical evaluation. A combined analytical-numerical solution is proposed and comparison with purely numerical solution is made.

## 2 Analytical Electromagnetic Field Evaluation

At uniform distribution of current density  $\delta$ , the vertical component of magnetic field for a solitary rectangular bar results with Biot-Savart law [2] (fig. 1):

$$H_y(x, y) = \frac{\delta}{2\pi} \left[ (x + a_1) \left( \operatorname{arctg} \frac{y + b_1}{x + a_1} - \operatorname{arctg} \frac{y - b_1}{x + a_1} \right) - (x - a_1) \left( \operatorname{arctg} \frac{y + b_1}{x - a_1} - \operatorname{arctg} \frac{y - b_1}{x - a_1} \right) + \frac{(y + b_1)}{2} \ln \frac{(x + a_1)^2 + (y + b_1)^2}{(x - a_1)^2 + (y + b_1)^2} - \frac{(y - b_1)}{2} \ln \frac{(x + a_1)^2 + (y - b_1)^2}{(x - a_1)^2 + (y - b_1)^2} \right] \quad (1)$$

In the case of two parallel bars, carrying the direct current  $I_0$ , the magnetic field ratio  $\eta$  in the points A and B can be deduced with superposition theorem (fig. 2):

$$\eta = \left| \frac{H_B}{H_A} \right|, \quad H_A = H_{1A} + H_{2A}, \quad H_B = H_{1B} - H_{2B} \quad (2)$$

At the beginning of a current step, the bar current can be considered distributed between two superficial vertical sheets and the magnetic fields modules ratio  $\eta_0$  is given by the currents ratio in the two sheets, considering the condition of zero magnetic field in the middle of the bar [2]:

$$\eta_0 = \left| \frac{H_B}{H_A} \right| = \frac{I_B}{I_A} = \frac{\operatorname{arctg} \frac{h}{b} - \operatorname{arctg} \frac{h}{2a+b}}{\operatorname{arctg} \frac{h}{b} + \operatorname{arctg} \frac{h}{2a+3b}}, \quad I_0 = I_A + I_B \quad (3)$$

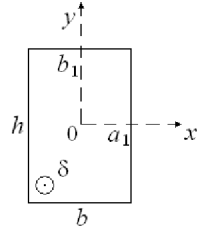


Fig. 1: Solitary bar.

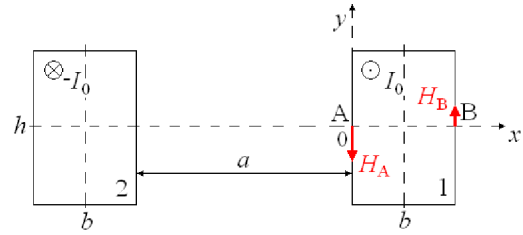


Fig. 2: System of two parallels bars.

More exactly, can be proposed the following formula, which depends on the  $\eta$  in direct current:

$$\eta'_0 = \frac{\operatorname{arctg}\left(\frac{1+\eta}{2} \cdot \frac{h}{b}\right) - \operatorname{arctg}\left(\frac{h}{2a + \frac{2b}{1+\eta}}\right)}{\operatorname{arctg}\left(\frac{1+\eta}{2\eta} \cdot \frac{h}{b}\right) + \operatorname{arctg}\left(\frac{h}{2(a+b) + \frac{2b}{1+\eta}}\right)} \quad (4)$$

In the case of current step injection  $i(t) = I_0 \cdot 1(t)$ , the Maxwell equations satisfied by electric and magnetic field are solved in [2] for the thin bars using Laplace transform. The magnetic field on the two lateral sides and the solution of field equations in central part of conductor are:

$$H_A \approx \frac{I_0}{(1+\eta)(h+b)}; \quad H_B = \eta H_A \quad (5)$$

$$H_y(\xi, \theta) = H_A \cdot \left[ \xi(1+\eta) - 1 + \frac{2}{\pi} \sum_{k=1}^{\infty} (-1)^k \frac{\eta \sin(k\pi\xi) - \sin(k\pi(1-\xi))}{k} e^{-(k\pi)^2\theta} \right] \quad (6)$$

$$E_z(\xi, \theta) = \frac{E_0}{1+\eta} \cdot \left[ 1 + \eta + 2 \sum_{k=1}^{\infty} (-1)^k [\eta \cos(k\pi\xi) + \cos(k\pi(1-\xi))] e^{-(k\pi)^2\theta} \right] \quad (7)$$

where  $\xi = \frac{x}{b}$ ,  $\theta = \frac{t}{\tau}$ ,  $\tau = \mu \sigma b^2$ ,  $E_0 = \frac{I_0}{\sigma b h} \approx \frac{1+\eta}{\sigma} \left( \frac{1}{b} + \frac{1}{h} \right) H_A$  (8)

For a voltage step application  $u(t) = U_0 \cdot 1(t)$ , assuming the approximation (5), the solution are:

$$H_y(\xi, \theta) = H_0 \cdot \left[ \xi - \frac{1}{1+\eta} - 2m \sum_{k=1}^{\infty} \frac{\eta \sin(v_k \xi) - \sin(v_k(1-\xi))}{v_k^2 ((m+1) \sin(v_k) + v_k \cos(v_k))} e^{-v_k^2 \theta} \right] \quad (9)$$

$$E_z(\xi, \theta) = E_0 \cdot \left[ 1 - 2m \sum_{k=1}^{\infty} \frac{\eta \cos(v_k \xi) + \cos(v_k(1-\xi))}{v_k ((m+1) \sin(v_k) + v_k \cos(v_k))} e^{-v_k^2 \theta} \right] \quad (10)$$

where  $m = \frac{\tau}{\tau_{\text{ext}}}$ ,  $\tau_{\text{ext}} = \frac{l_{\text{ext}}}{r_0}$ ,  $I_0 = \frac{U_0}{r_0}$ ,  $r_0 = \frac{2z}{\sigma b h}$ ,  $l_{\text{ext}} \approx \frac{\mu_0 a z}{h}$ ,  $H_0 = \frac{I_0}{h}$  (11)

and  $v_k$  verify the equation:  $m(\eta + \cos v_k) = v_k \sin v_k$  (12)

### 3 Numerical Electromagnetic Field Evaluation

The numerical simulation of transient electromagnetic field at current step injection and voltage step application to short-circuited high-enough bars has been obtained with finite element method using the FLUX 2D program developed by CEDRAT Company and Grenoble Electrical Engineering Laboratory.

The bars system was modelled with massif conductor components connected to the step signals via Circuit Coupling module. The choice of the rate  $h/b$  equal to 30 (fig. 2) corresponds well to assumption made in [2] of high-enough bars. The distance  $a$  between the bars was considered equal to  $2b$ . A quarter of the model was analysed, a four time reduction of the nodes number being obtained.

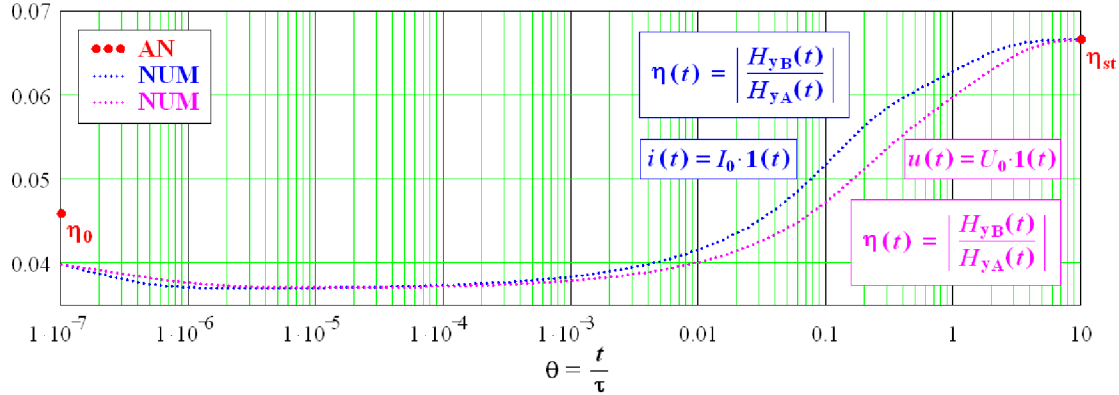


Fig 3: Evolution of the ratio  $\eta$  along the transient process at current and voltage step signals application

The time analysis assumes a string of static analysis, serially depending each other. The accuracy of simulation depends on the thinness of mesh, both in space and in time. The thinness must be imposed in the zones with strong variations of quantities – along the bars sides for the spatial mesh and towards the beginning of transient process.

The transient numerical simulation begins at the moment corresponding to  $\theta = 10^{-7}$  with the minimum time step allowed by the program ( $p = 10^{-9}$  s). This is increased in steps, on little time intervals till the end of transient process, practically corresponding to  $\theta = 10$ . Totally, 234 time values were analysed.

The way of variation time mesh has also an important influence on the accuracy. Thus, the step time has been increased along the simulation such as its variation does not exceed 2-2.5 times at the homogeneous time intervals junctions.

In the figure 3 is shown the numerical evolutions in time of ratio  $\eta$  along the transient process at current and voltage steps. The initial and final values calculated with (3) or (3') and (2) are also designed. The coincidence of analytical and numerical results is evident at the end of process. The negative slope of the numerical curves on the first two decades is probably due to the transient process of computation method.

The numerical results of magnetic field penetration and of the current density distribution in conductors were obtained for some moments corresponding to  $\theta$  between 0.001 and 1, at current and voltage step. In [2], the tangential component of magnetic field and longitudinal component of electric field were analytically evaluated using the equations (6)-(12), considering the ratio  $\eta$  of static magnetic field for all analysed moments. In this paper a combined analytic-numerical solution is proposed, using the same equations with the ratio  $\eta$  coming from numerical simulation (fig. 3). The solutions  $v_k$ , of equation (12), have been numerically evaluated using MATHCAD program.

In figures 4-7 can be seen the results of numerical simulation compared to analytical and mix analytical-numerical solutions at current step injection. There's agreement can be observed.

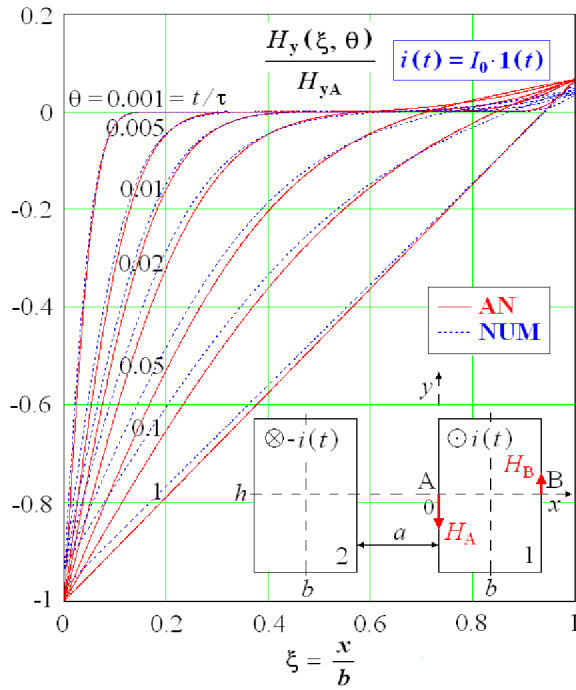


Fig 4: Numerical and analytical results of transient magnetic field in conductor 1 at current step injection, for  $h/b = 30$  and  $a/b = 2$ .

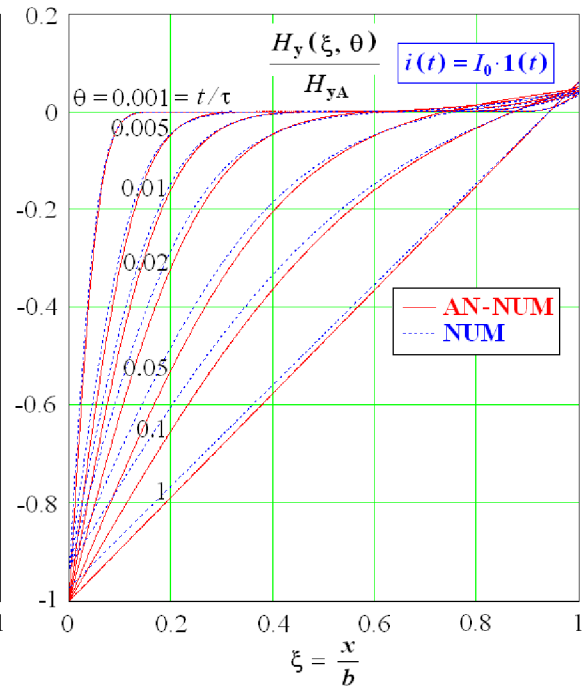


Fig 5: Numerical and mix analytical-numerical results of transient magnetic field in conductor 1 at current step injection, for  $h/b = 30$  and  $a/b = 2$ .

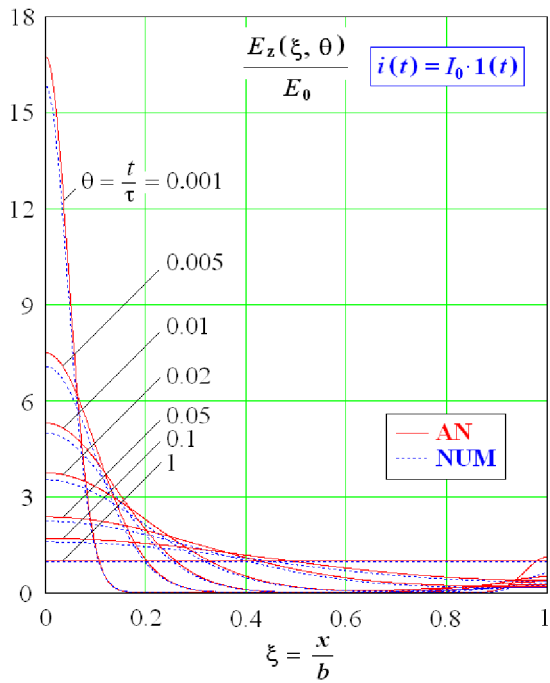


Fig 6: Numerical and analytical results of transient electric field in conductor 1 at current step injection, for  $h/b = 30$  and  $a/b = 2$ .

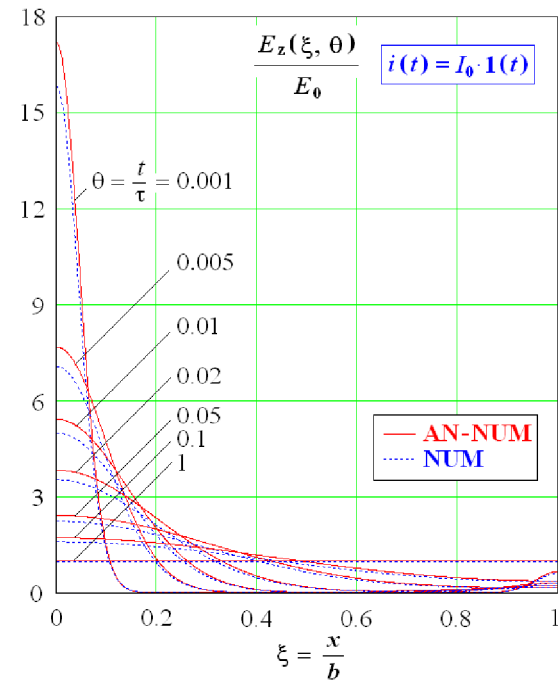


Fig 7: Numerical and mix analytical-numerical results of transient electric field in conductor 1 at current step injection, for  $h/b = 30$  and  $a/b = 2$ .

In figures 8-11 can be seen the results of numerical simulation compared to analytical and combined analytical-numerical solutions at voltage step application, in best agreements.

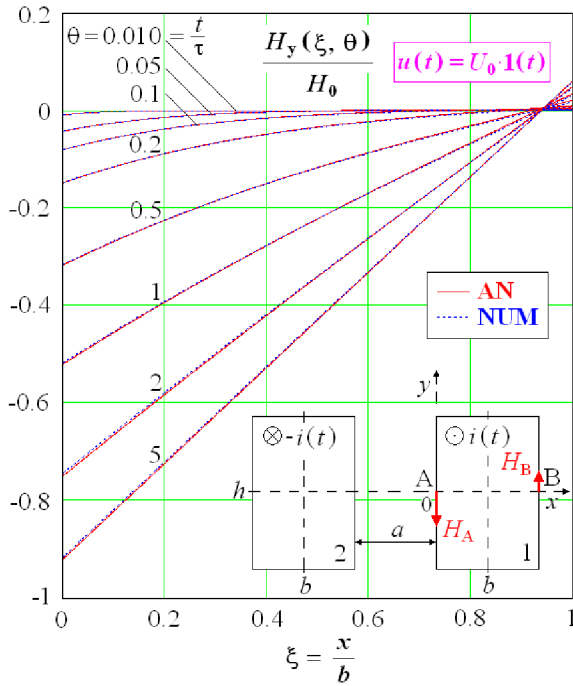


Fig 8: Numerical and analytical results of transient magnetic field in conductor 1 at voltage step application, for  $h/b = 30$  and  $a/b = 2$ .

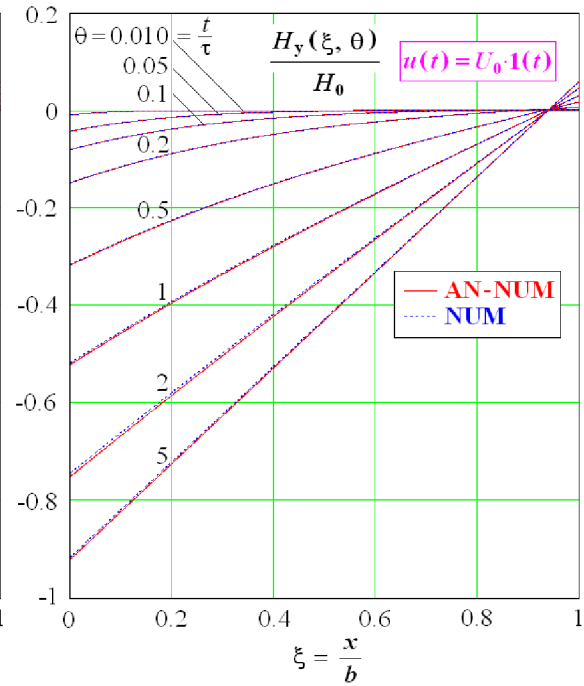


Fig 9: Numerical and mix analytical-numerical results of transient magnetic field in conductor 1 at voltage step application, for  $h/b = 30$  and  $a/b = 2$ .

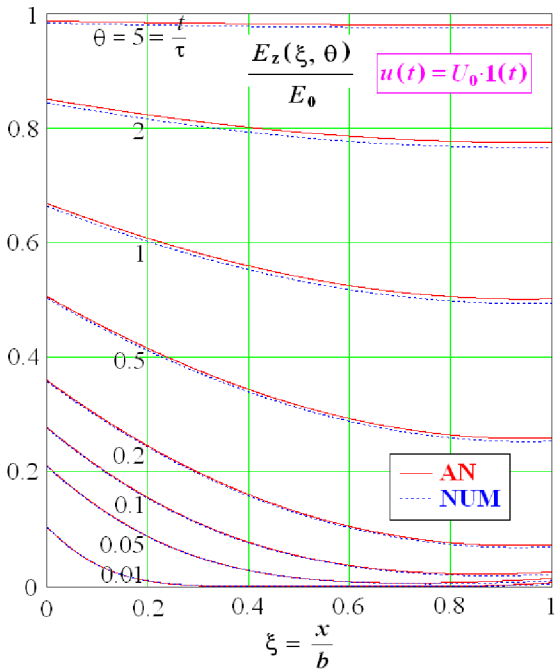


Fig 10: Numerical and analytical results of transient electric field in conductor 1 at voltage step application, for  $h/b = 30$  and  $a/b = 2$ .

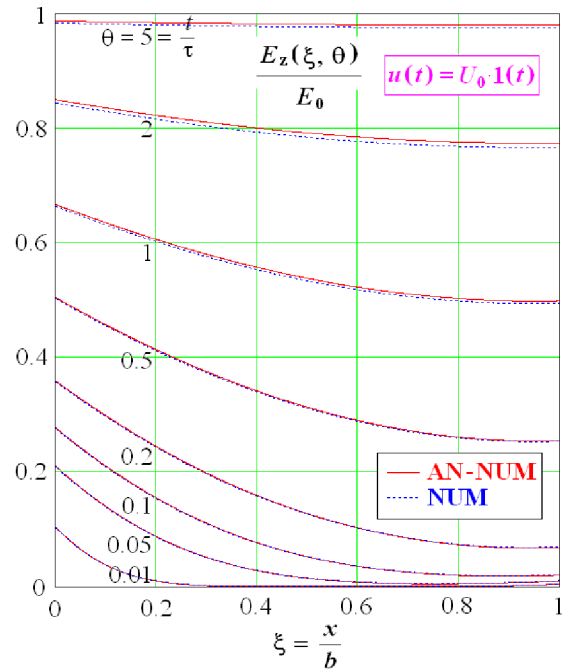


Fig 11: Numerical and mix analytical-numerical results of transient electric field in conductor 1 at voltage step application, for  $h/b = 30$  and  $a/b = 2$ .

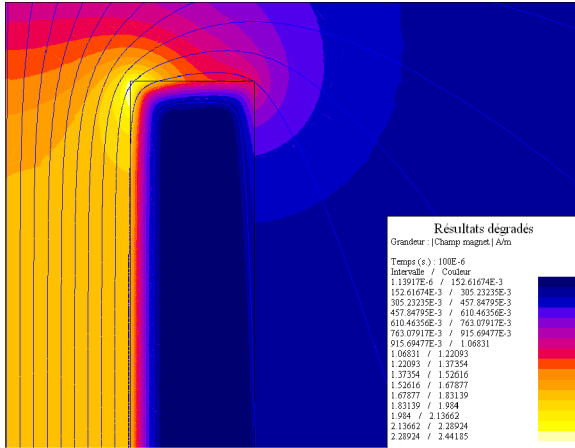


Fig 12: Magnetic field distribution at  $\theta = 10^{-2}$  for current step injection.

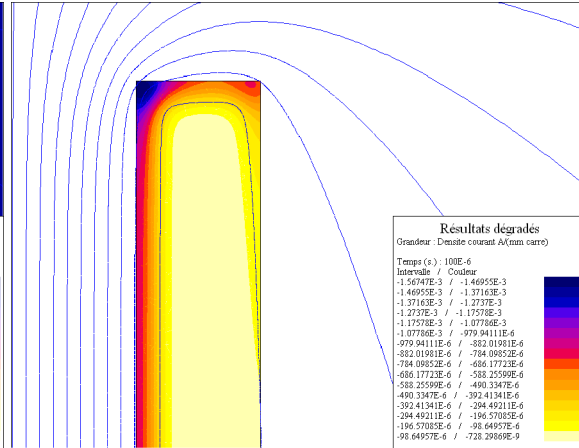


Fig 13: Current density distribution at  $\theta = 10^{-2}$  for current step injection.

Using visualisation facilities offered by FLUX postprocessor, in the figures 12 and 13 are presented the magnetic field and the current density distributions in the studied domain for  $\theta = 10^{-2}$  in the case of current step injection.

#### 4 Conclusions

- The transient electromagnetic field in and around a system of two non-magnetic homogenous rectangular bars is evaluated with finite element method using FLUX 2D program. For high-enough bars, good agreement with old analytical solution was found.
- Thinness mesh in the zones with strong variations of quantities and uniformly time mesh variation insure a good accuracy of results.
- A combined analytical-numerical solution for the field penetration in high-enough bar and for the time variation of the current density distribution in bars was proposed and its agreement with purely numerical evaluation has been established.

#### References

- [1] A. Țugulea. *Transitory electromagnetic field in massive bus bars* (In Roumanian), St. cerc. Energ. Electr., tom 22, no. 1, Bucharest, 1972, pp. 67-93.
- [2] G.A. Cividjian. *Current distribution in rectangular bus bars*, Revue Roumaine des Sciences Electrotechnique et Energétiques, Vol. 48, No. 2/3, Bucharest, 2003, pp. 313–320.
- [3] FLUX 9.3.2. *User's guide*.

**Acknowledgments** - The authors thank to the CEDRAT Company for the rights to use the FLUX software, which has allowed the numerical simulation.